

SUPPORTING INFORMATION

Industrial lignins as efficient biosorbents for Cr(VI) water remediation: transforming a waste into an added value material

Marianna Vescovi,^a Matteo Melegari,^a Cristina Gazzurelli,^a Monica Maffini,^a Claudio Mucchino,^a Paolo Pio Mazzeo,^a Mauro Carcelli,^a Jacopo Perego,^b Andrea Migliori,^c Giuliano Leonardi,^d Suvi Pietarinen,^e Paolo Pelagatti ^{*a,f†} and Dominga Rogolino, ^{*a†}

^a*Department of Chemistry, Life Sciences and Environmental Sustainability, University of Parma, Parco Area delle Scienze 17/A, 43124 Parma, Italy*

^b*Dipartimento di Scienza dei Materiali, Università degli Studi Milano-Bicocca, Milan, Italy.*

^c*CNR-IMM Sezione di Bologna, via Gobetti 101 - 40129 Bologna, Italy*

^d*Green Innovation GMBH, 6020, Innsbruck, Austria*

^e*UPM-Kymmene Oyj, Alvar Aallon katu1, FI-00101 Helsinki, Finland*

^f*Interuniversity Consortium of Chemical Reactivity and Catalysis (CIRCC), via Celso Ulpiani 27, 70126 Bari, Italy*

[†] *Authors equally contributed to the work.*

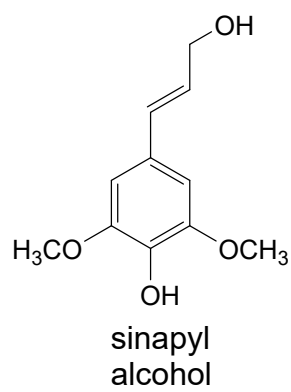
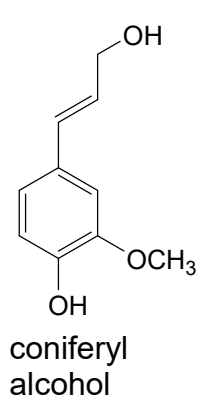
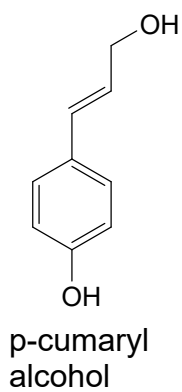
Inductively Coupled Plasma Atomic Emission Spectroscopy (ICP-AES). For solid samples, 5 - 15 mg were suspended in 5 mL of HNO₃ 65% and 1 mL of H₂O₂ 30%, then digested in a Milestone microwave MLS-1200 MEGA (digestion sequence: 1 min at 250-Watt, 1 min at 0-Watt, 5 min at 250-Watt, 5 min at 400-Watt, 5 min at 650-Watt, 5 min of cooling). Those solutions were diluted to 50 mL with bi-distilled water. For liquid samples, the solutions were either analyzed as they were or diluted 1:2 with bi-distilled water and 1:100 with 10% HNO₃ for the Zn solutions and analyzed using an emission spectrometer JY 2501 with coupled plasma induction in radial configuration HORIBA Jobin Yvon (Kyoto, Japan), ULTIMA2 model. Instrumental features: monochromator Model JY 2501; focal length 1 m; resolution 5 pm; nitrogen flow 2 L/min. ICP source: nebulizer Meinhard, cyclonic spraying chamber; argon flow 12 L/min; wavelengths range 160-785 nm; optical bench temperature 32 °C. The wavelength used for quantitative analysis was chosen by examining the emission line with greater relative intensity, ensuring that there was no spectral interference with the Argon emission lines. Acquisition parameters: wavelength Fe(nm); Cr (nm): 267.716. Voltage (V): 580; gain: 100. The quantitative analysis was performed after the acquisition of a calibration line using standard solutions in HNO₃ 10% for the solid samples and water for solutions to simulate the final acidity of the samples. The concentration range of the standards varied from 0.05 mg/L to 50 mg/L of Fe and 0.05 mg/L to 70 mg/L of Cr. Data acquisitions and processing were performed using the ICP JY v 5.2 software (Jobin Yvon). Measurements were performed in triplicate.

UV-Visible measurements. UV-visible spectra of the Cr(VI)-DPC solutions systems were collected with a Lambda 465 (PerkinElmer) Diode Array spectrophotometer equipped with a Peltier Control (PerkinElmer) using the 8-position cell changer as sample holder. 1 cm path length quartz cuvettes were used in all experiments. The analyzed solutions were prepared by dilution of the Cr(VI) containing supernatants of the lignin reduction tests. The 1,5-diphenyl carbazide (DPC, minimum purity 98 %) solution was prepared as follows: 20 mg of 1,5-diphenylcarbazine were dissolved in 20 ml of ethanol (95 %) (solution A). In a 250 ml flask, 75 mL of 85% H₃PO₄ were added, and the volume was brought to 250 mL with distilled water (solution B). The final solution (C) was obtained

by slow addition of 20 mL of the DPC solution to 80 mL of the H_3PO_4 solution. This solution stored at 4°C could be used within 3-4 days. The spectra were collected in the 200–800 nm range and the calculations for the Cr(VI) concentrations were done taking in consideration only the intensity at $\lambda = 540$ nm (maximum absorption of the Cr(VI)-DPC adduct). To prepare the solutions for the analysis, 1:10 of the total volume of the final solution was composed by solution C. The rest was composed by the diluted Cr(VI) solution (dilution factors 1:2.5, 1:20 and 1:100) to reach a final concentration of Cr(VI) in the range of 0.02 and 0.4 ppm (linearity interval of the technique). Calibration lines were prepared each time the sample solutions were analyzed. Those solutions were obtained in the same way as the samples but using a 5-ppm stock solution of $\text{K}_2\text{Cr}_2\text{O}_7$ obtaining final samples with concentrations of 0.02, 0.05, 0.10, 0.20, 0.30 and 0.40 ppm. Linear regressions of the point of the calibration lines was performed using the Origin program.

Scheme S1. Structural scheme of the three monolignols of lignin

Lignin monolignols



Lignin structural units

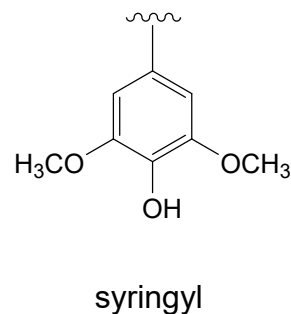
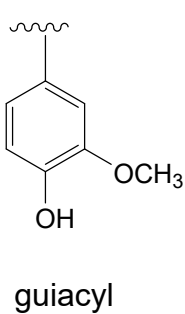
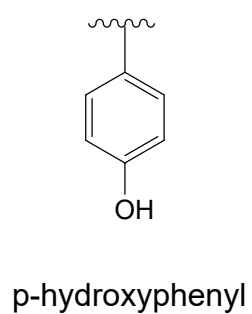


Figure S1. $^{31}\text{P}\{^1\text{H}\}$ -MAS-NMR spectrum of P_LIG.

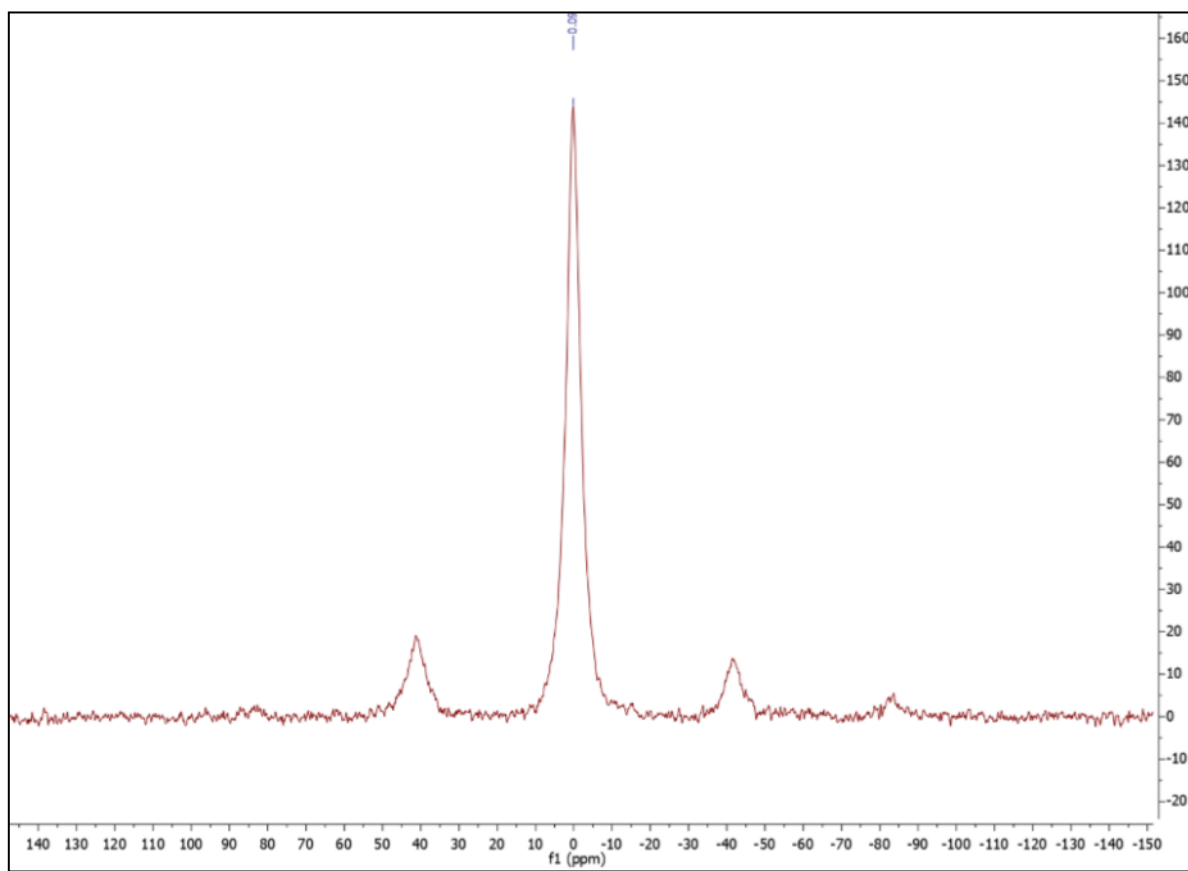


Figure S2. Solid state $^{13}\text{C}\{^1\text{H}\}$ -NMR of HMW (green) and P-Lig (red).

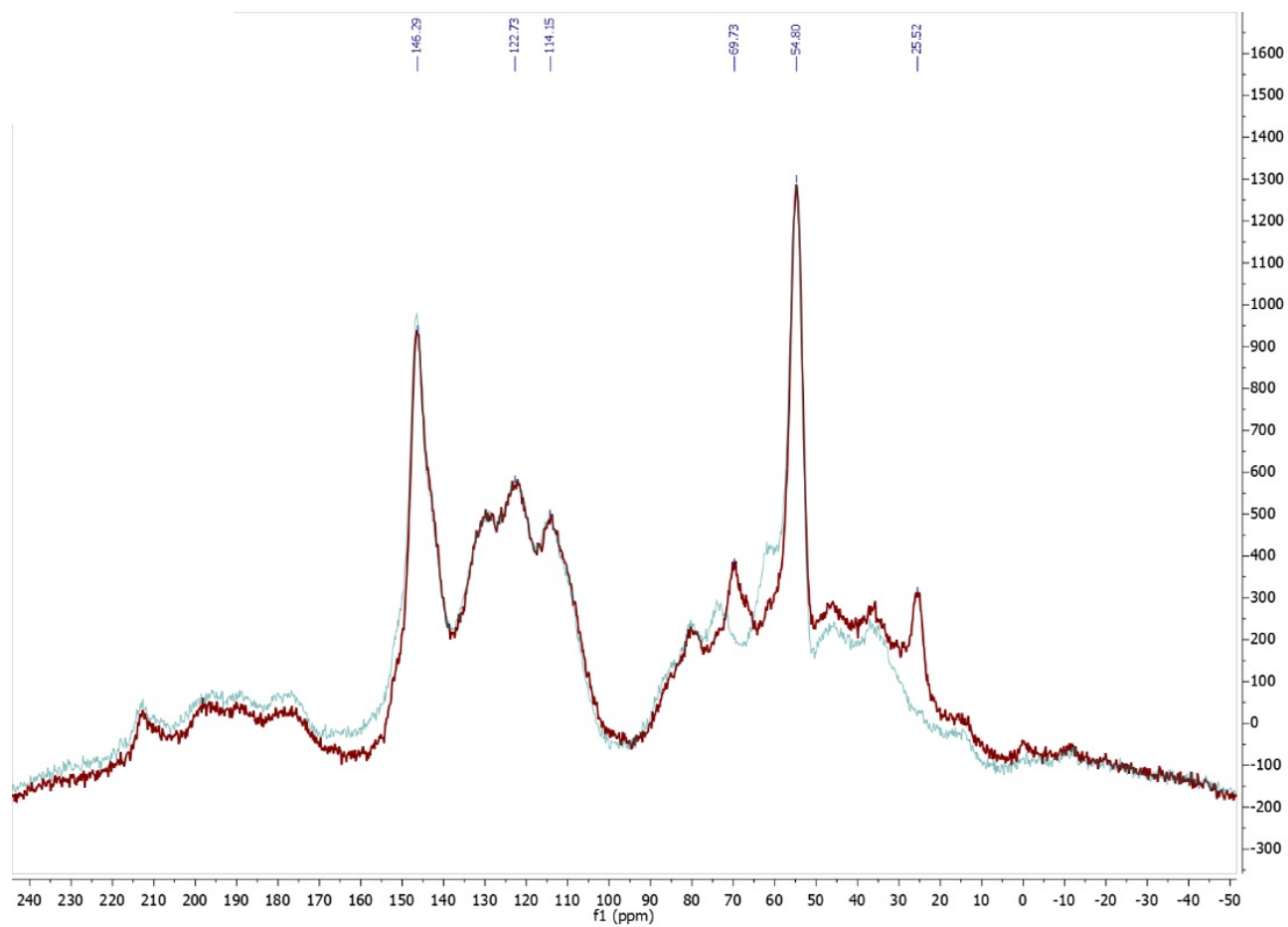


Figure S3. EDS analysis and EDS mapping for P-Lig, phosphorous is represented in red.

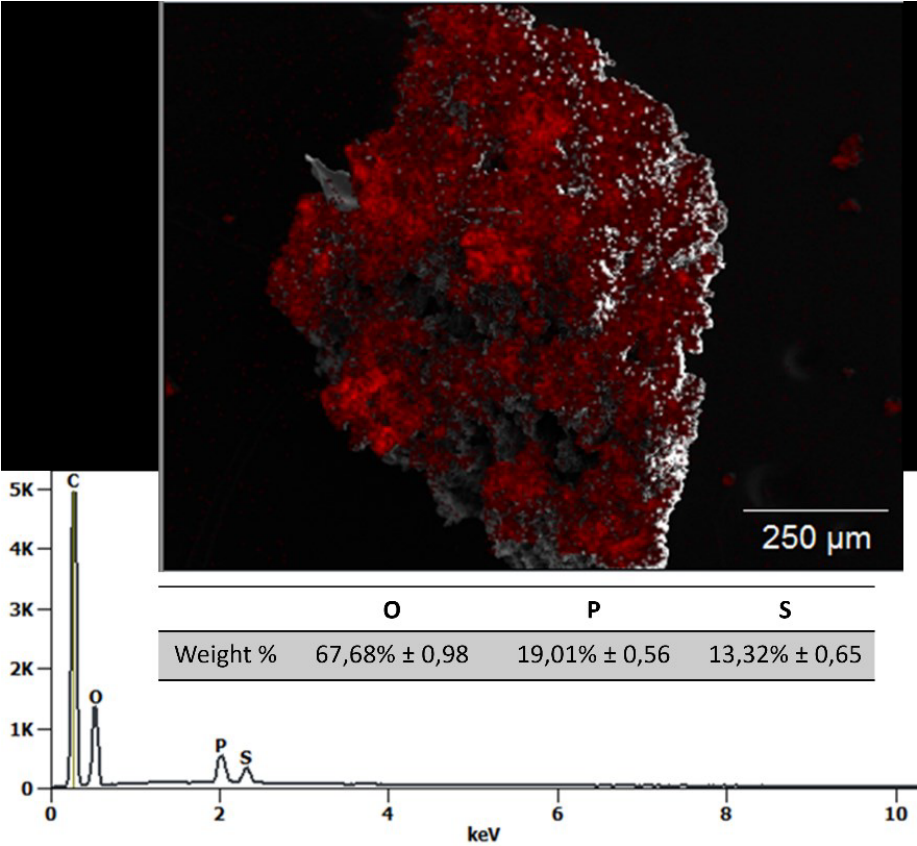


Figure S4. TGA profiles of HMW (blue) and P_Lig (red).

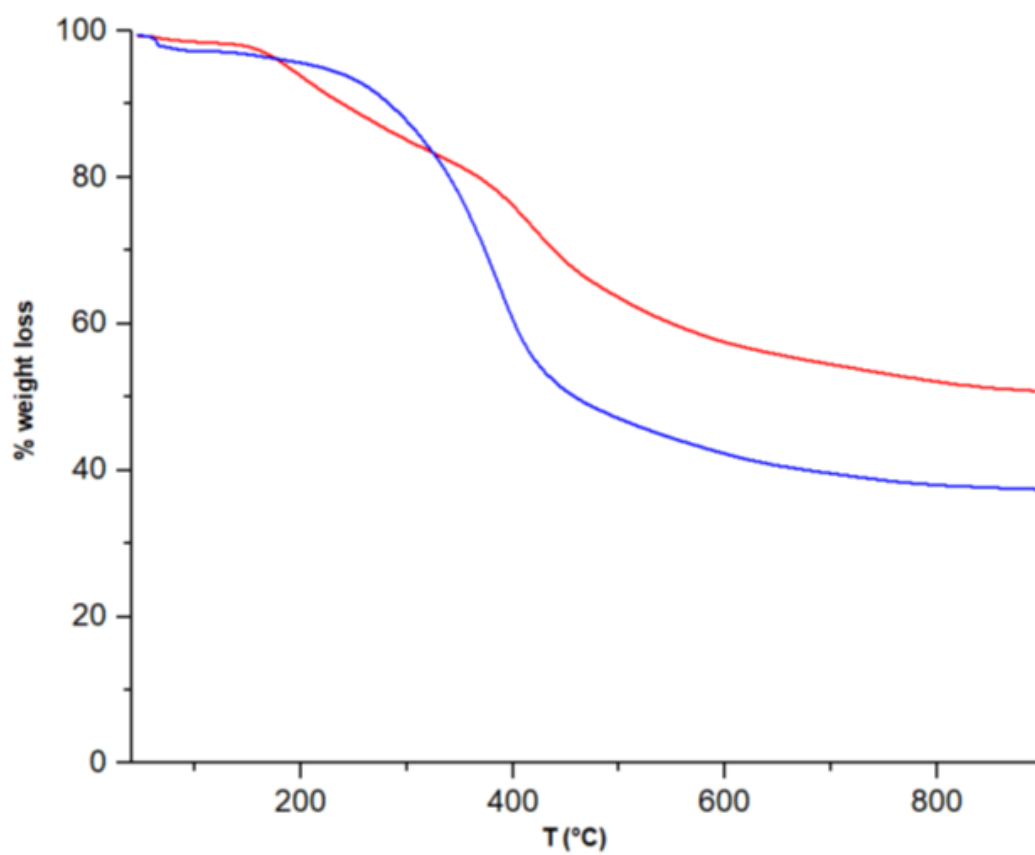


Figure S5. FTIR spectra of HMW (red) and Ac-Lig (purple).

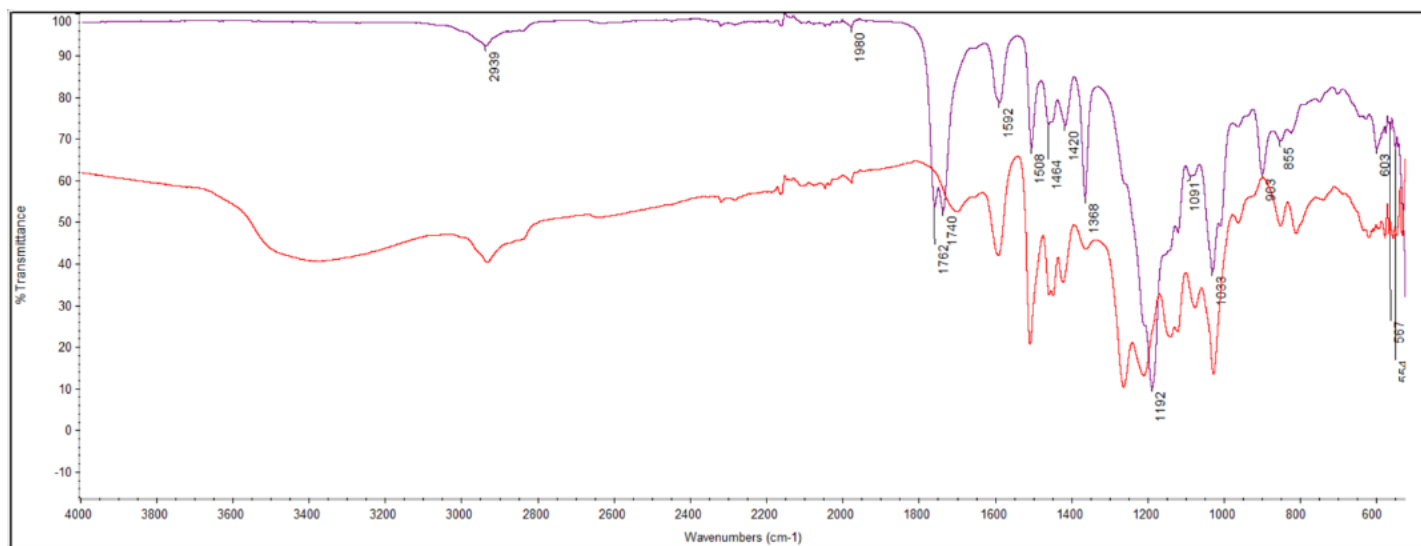


Figure S6. $^{13}\text{C}\{^1\text{H}\}$ NMR spectrum of Ac-Lig in DMSO-d_6 .

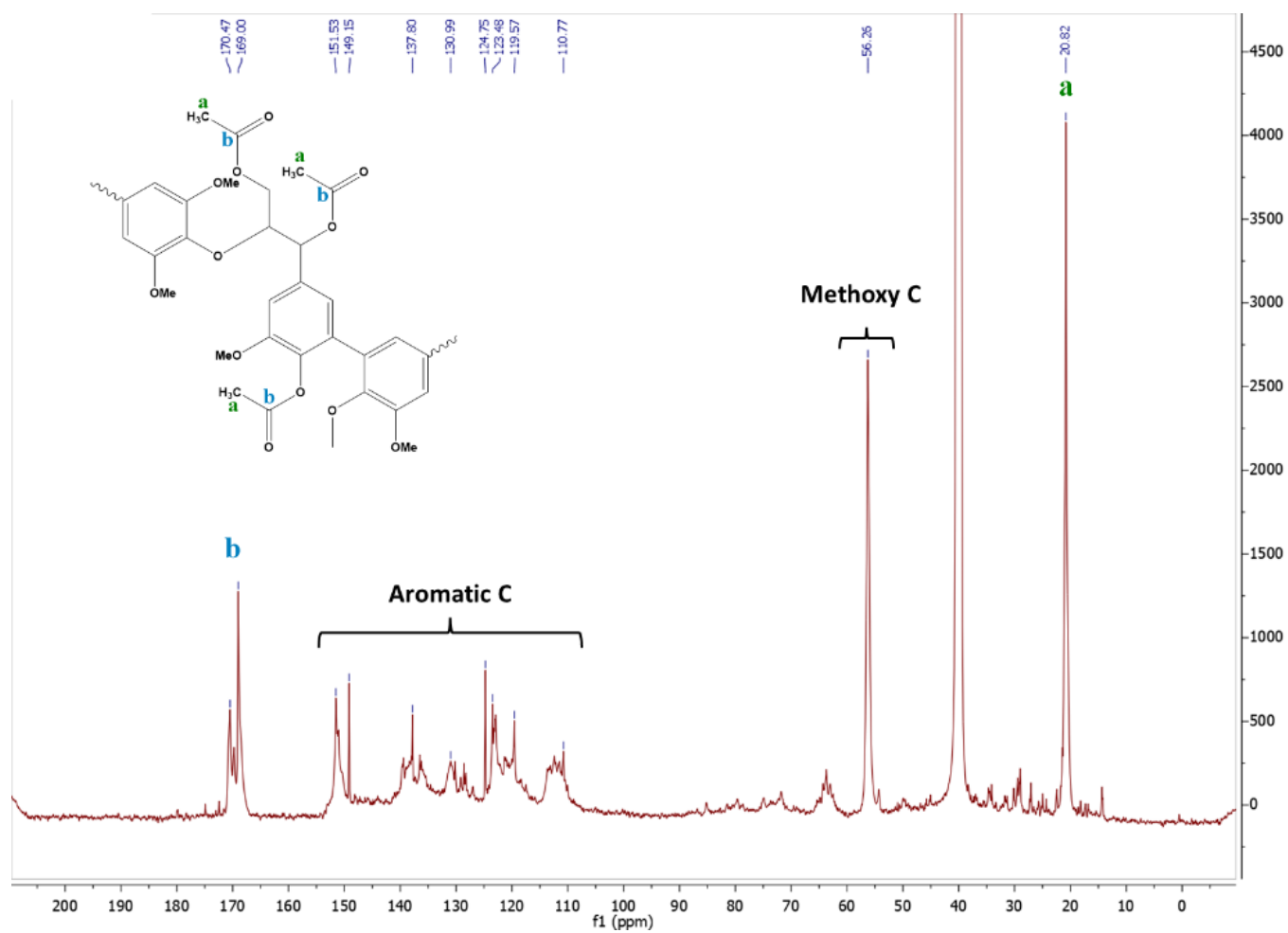


Figure S7. SEM images of A) HMW, and B) Ac-Lig

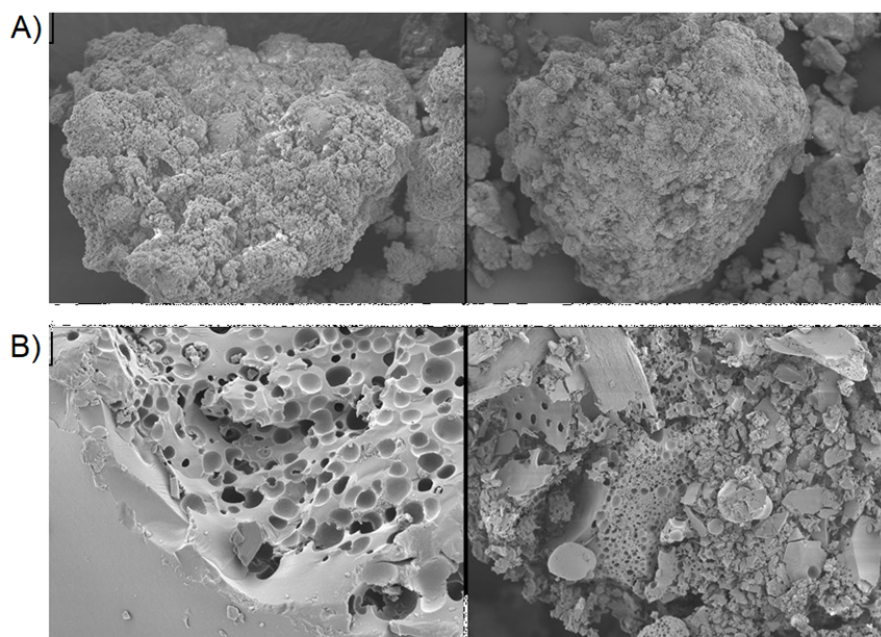


Figure S8. Pawley fit (red line) of the experimental PXRD pattern of lignin@goethite (black line). Blue sticks shown the refined positions of goethite Bragg peaks. Differential pattern ($Y_{\text{obs}} - Y_{\text{cal}}$) is also reported. Iron content $\approx 10\%$.

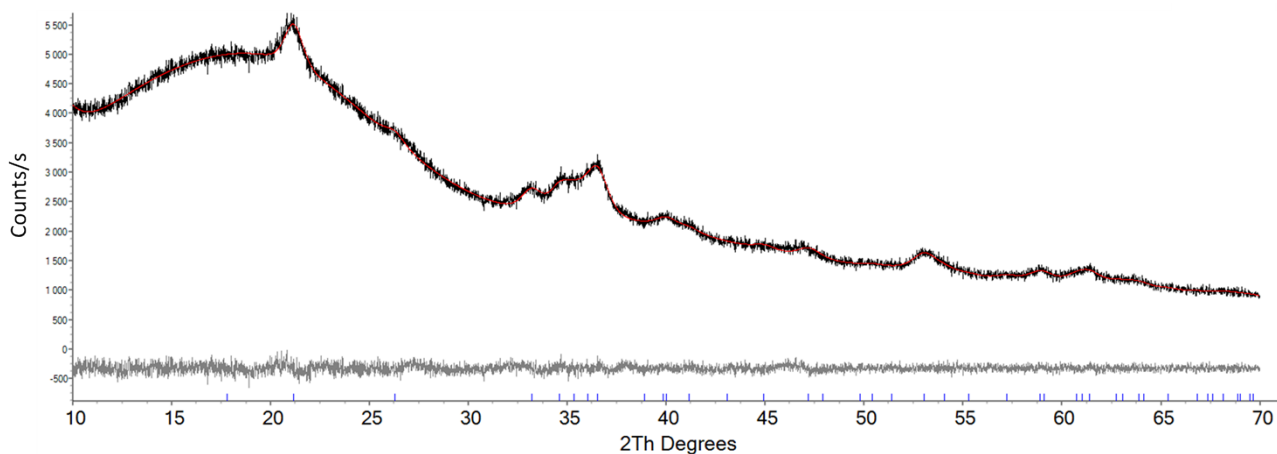
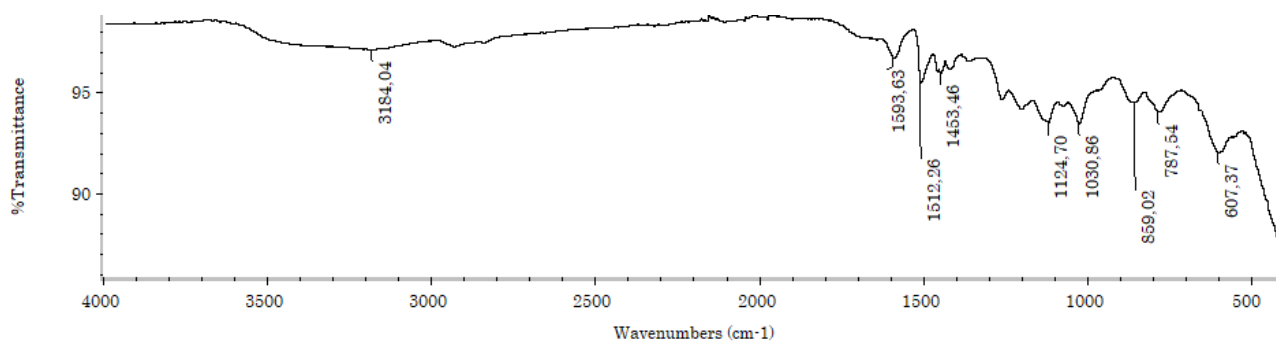


Figure S9. Infrared spectrum of lignin@goethite.



The IR characterization of goethite can be found in *Journal of Experimental Nanoscience* **2013**, *8*, 869-875, doi: <http://dx.doi.org/10.1080/17458080.2011.616541>.

Figure S10. A) STEM-HAADF images of lignin@goethite hybrid material. The goethite crystals appear brighter than the lignin matrix. Crystals have elongated form with length in the range 30-80 nm and thickness in the range 10-20 nm. Rounded clusters are present, with a size between 10 and 30 nm. B) X-ray microanalysis on both elongated crystals and rounded clusters confirms the presence of iron. Electron diffraction on selected area mainly corresponds to the presence of Goethite.

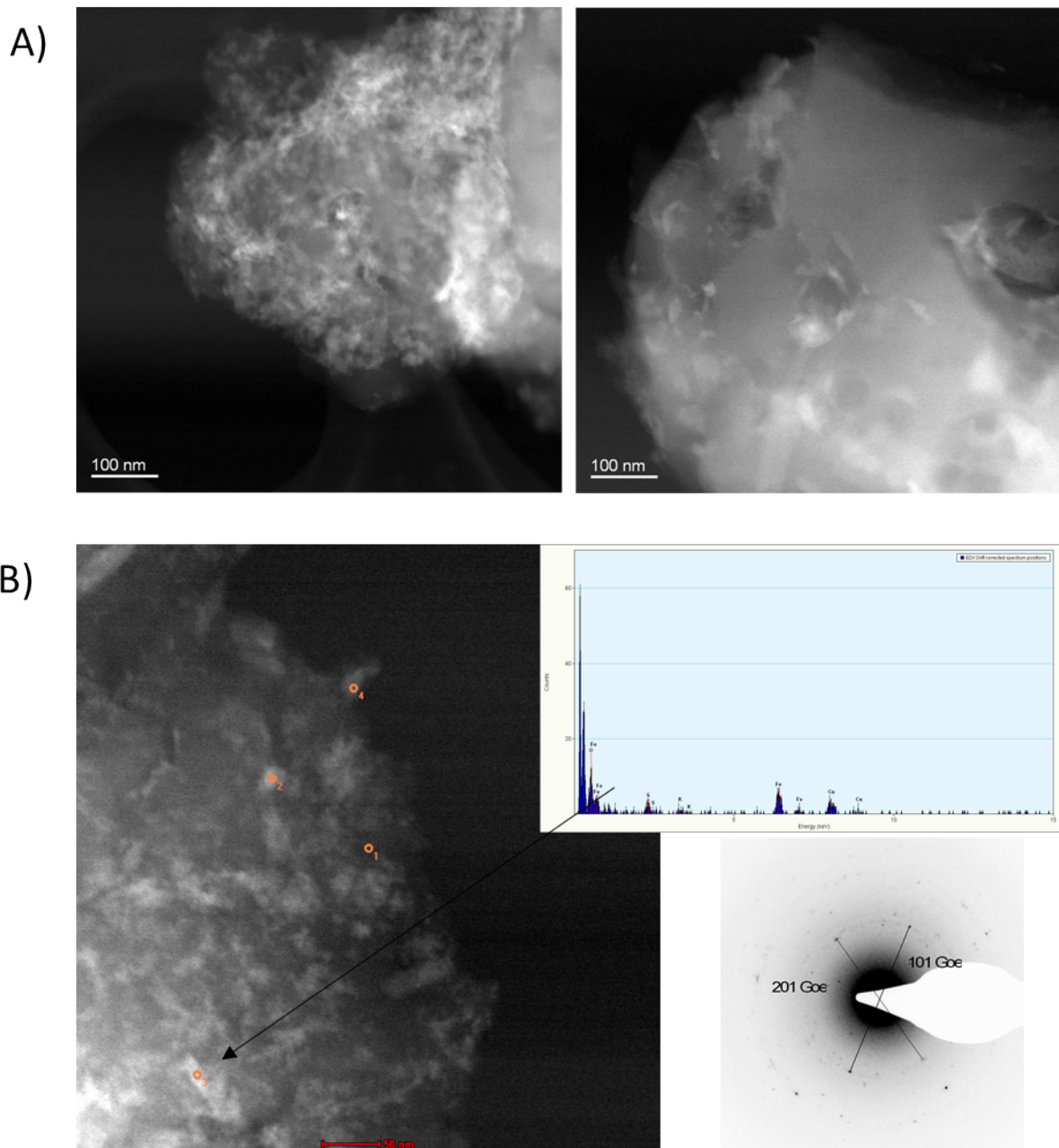


Figure S11. Pawley fit (red line) of the experimental PXRD pattern of lignin@magnetite (black line). Deconvolution of magnetite (blue line) and goethite (green line) contributions is emphasized. Blue and green sticks shown the refined positions of magnetite and goethite Bragg peaks respectively. Differential pattern (gray line; $Y_{\text{obs}} - Y_{\text{cal}}$) is also reported.

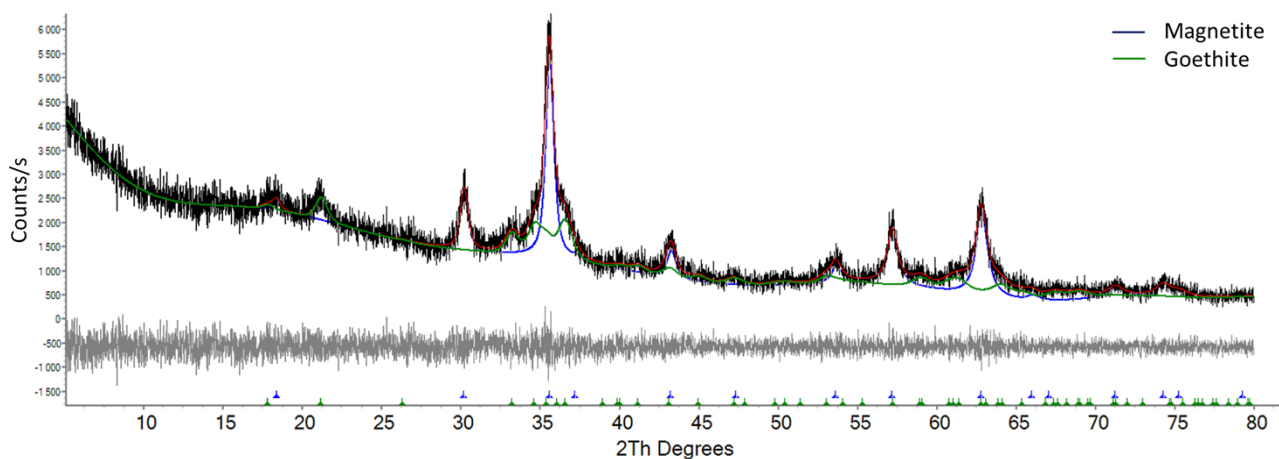
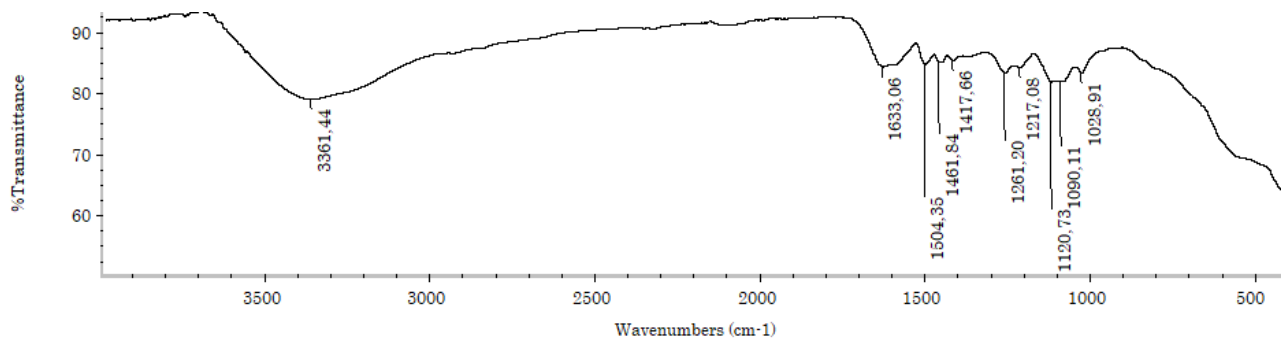


Figure S12. Infrared spectrum of lignin@magnetite.



The IR characterization of pure magnetite can be found in *Journal of Experimental Nanoscience* **2013**, 8, 869-875, doi: <http://dx.doi.org/10.1080/17458080.2011.616541>.

Figure S13. Pawley fit (red line) of the experimental PXRD pattern of magnetite (black line). Blue sticks shown the refined positions of magnetite Bragg peaks. Differential pattern ($Y_{obs} - Y_{cal}$) is also reported.

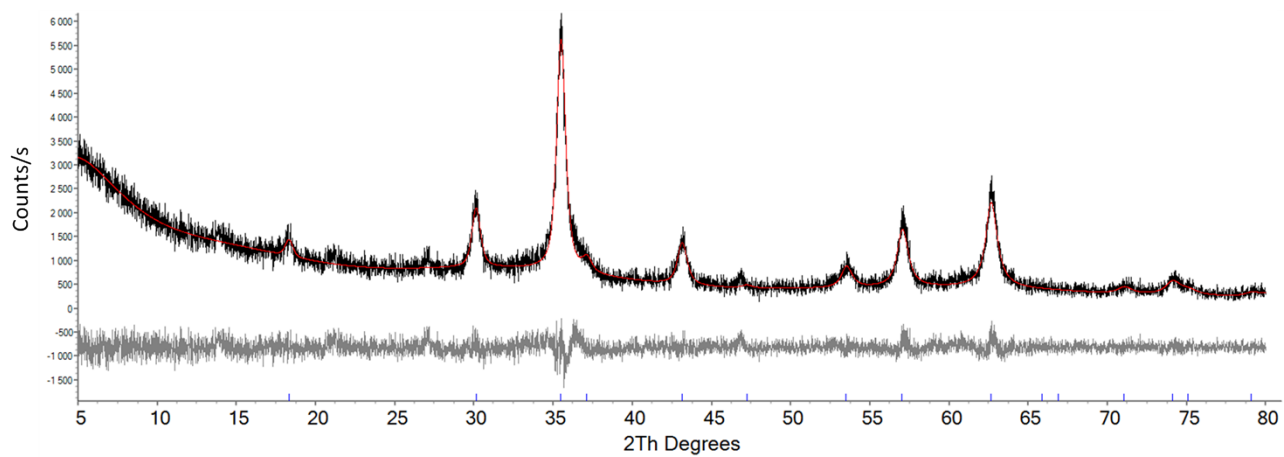


Figure S14. N₂ adsorption isotherms collected at 77 K up to 1 bar for sample HMW lignin (red circles), P-Lig (blue triangles) and Ac-Lig (violet diamonds).

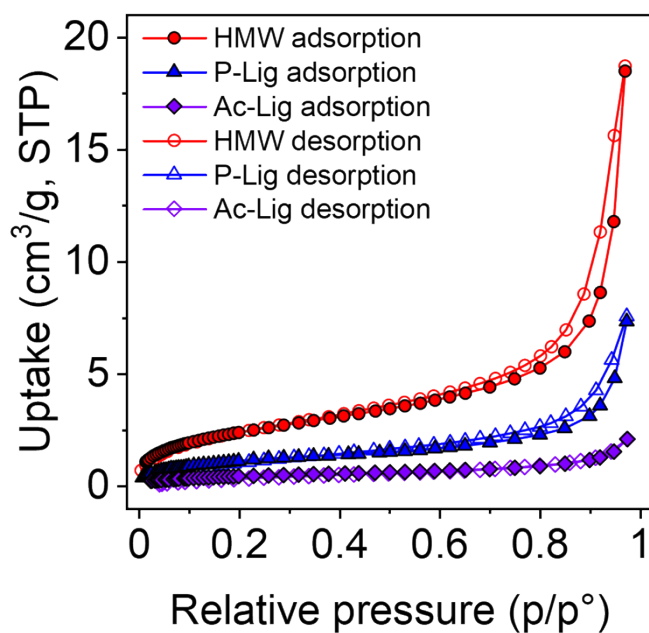


Figure S15. N₂ adsorption isotherms collected at 77 K up to 1 bar for sample HMW lignin (red circles), and EH (green diamonds).

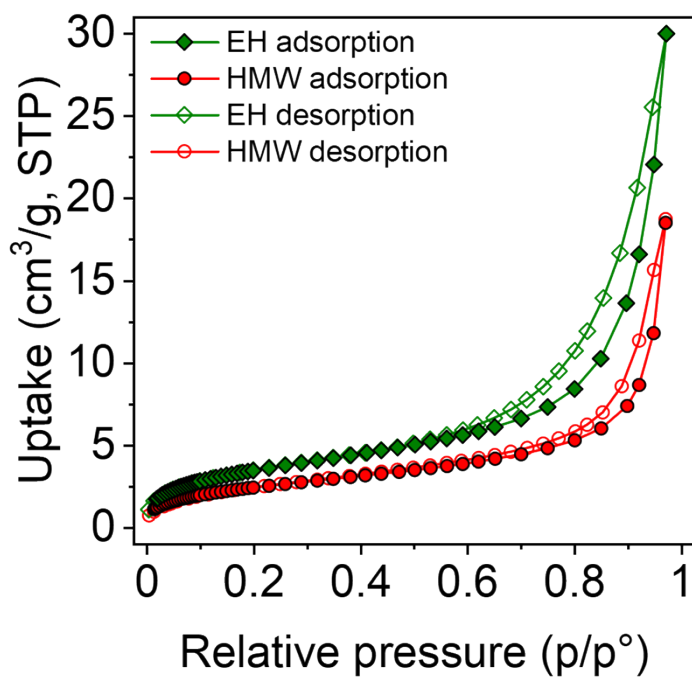


Figure S16. Reproducibility of the N₂ adsorption isotherms for EH sample. The first (green diamonds), second (blue triangles) and third adsorption isotherms (red crosses) of sample EH are displayed.

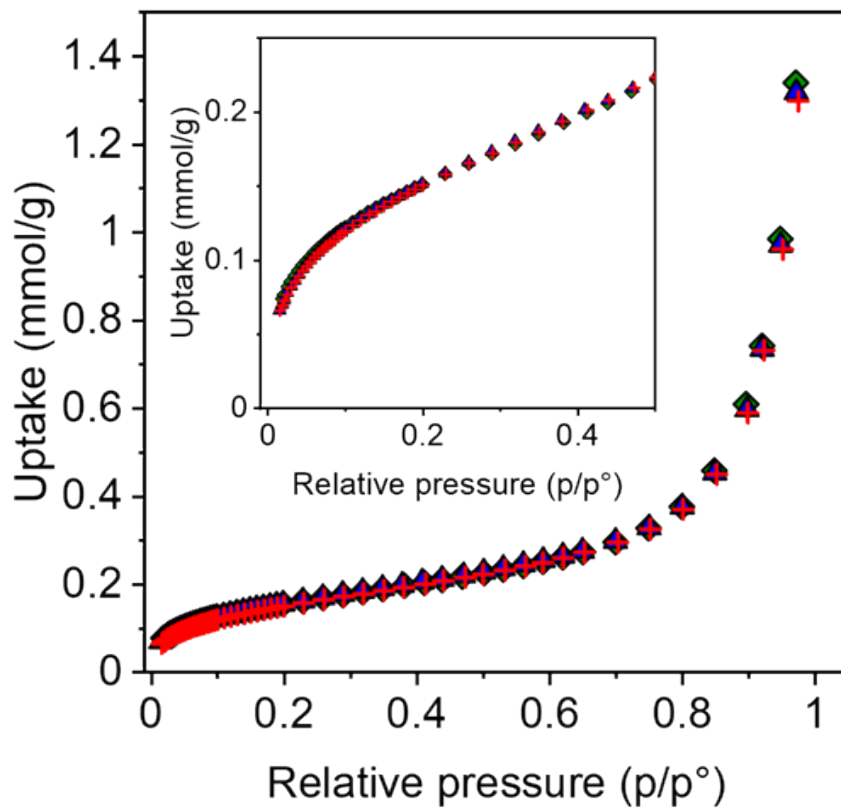


Figure S17. Effect of the use of different acids to adjust the pH of the solutions. The effect of the use of a 0.1 M solution of NaNO₃ and of tap water instead of distilled water in the preparation of the initial Cr(VI) solution is also reported. Red bars refer to the removal of Cr(tot) whereas the grey bars refer to the reduction of Cr(VI). pH = 2; 1 g/L of HMW, 5 mg/L of initial Cr(VI) concentration, 2h contact time.

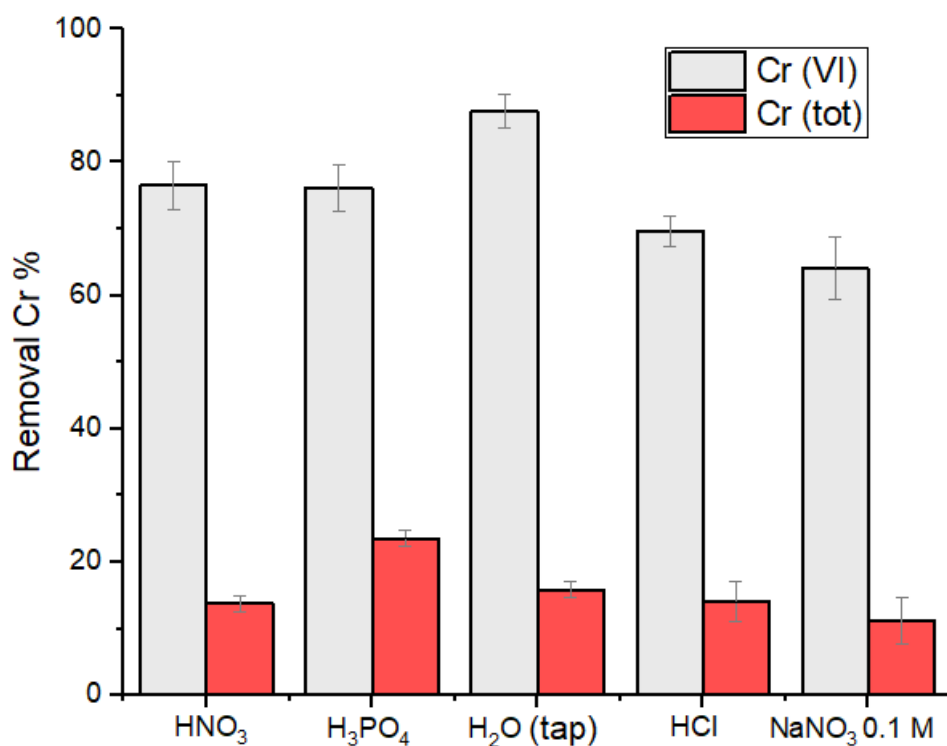


Figure S18. Fe leaching for the Cr(VI) removal experiments with Fe-containing adsorbents. Both the leaching in terms of final Fe concentration (grey on the left) and in terms of percentage leaching (blue on the right) are reported.

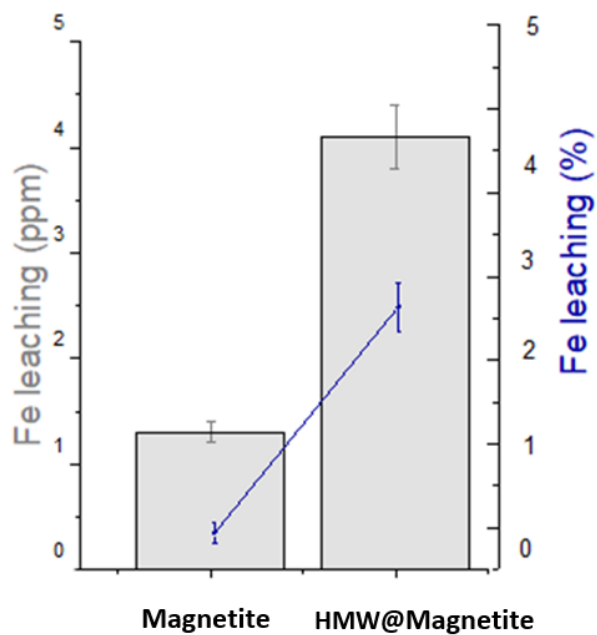


Table S1. BET and Langmuir surface areas of sample EH calculated from three different adsorption isotherms.

Sample	BET surface area (m ² /g)	Average BET surface area (m ² /g)	Langmuir surface area (m ² /g)	Average Langmuir surface area (m ² /g)
EH_run 1	12.8	12.87 ± 0.05	18.2	18.4 ± 0.2
EH_run 2	12.9		18.6	
EH_run 3	12.9		18.5	

Table S2. Elemental analysis results for P_LIG samples (triplicate).

	N	C	H	S
P-Lig1	0.14	60.44	5.65	1.56
P-Lig2	0.14	58.57	5.83	1.45
P-Lig3	0.14	60.78	5.69	1.54
HMW	0.13	63.28	6.66	1.91

Table S3. Removal percentage of Cr(VI) and total chromium for experiments performed at 5 ppm initial Cr(VI) concentration with 2 h contact time and 1 g/L of HMW.

pH	Cr(VI)		Cr(tot)	
	conc. (ppm)	removal (%)	conc. (ppm)	removal (%)
2	1.2 (±0.2)	77 (±4)	2.7 (±0.05)	38.3 (±1)
3	3.4 (±0.2)	33 (±4)	4.9 (±0.1)	3 (±1)
4	3.9 (±0.1)	23 (±2)	4.6 (±0.1)	8 (±2)

